Phase Separation and Surfactant Stratification in Styrene/*n*-Butyl Acrylate Copolymer and Latex Blend Films. 17. A Spectroscopic Study†

Yaqiu Zhao and Marek W. Urban*

Shelby F. Thames Polymer Research Center, School of Polymers and High Performance Materials, The University of Southern Mississippi, Hattiesburg, Mississippi 39406

Received April 12, 1999; Revised Manuscript Received December 10, 1999

ABSTRACT: These studies focus on behavior of sodium dioctylsulfosuccinate (SDOSS) surfactant molecules in styrerie/*n*-butyl acrylate (Sty/*n*-BA) copolymers and blended latexes. Using a combination of IR and Raman spectroscopic and microanalytical techniques, not only stratification of SDOSS surfactant molecules across latex film thickness can be assessed, but also the effect of latex composition on coalescence can be analyzed. For Sty/*n*-BA latex copolymers, SDOSS···H_20, SDOSS···COOH associations, and free SDOSS are formed at the film−air (F−A) interface and exhibit nonuniform distributions across the film thickness. However, for p-Sty/p-*n*BA latex polymer blends, SDOSS is distributed uniformly at the F−A interface, and its concentration levels are significantly lower when compared to Sty/*n*-BA copolymer latexes. These studies show that, while step-scan photoacoustic Fourier transform infrared (SS-PAS FT-IR) and attenuated total reflectance (ATR) FT-IR are effective depth profiling methods for latex. films, FT-IR and FT-Raman imaging techniques provide unique analytical facilities for typically nondistinguishable surface latex components.

Introduction

While a decade ago it was fashionable to minimize the amount of volatiles in polymer dispersions, today's environmental issues mandate that volatile organic content (VOC) is virtually diminished to zero. While elimination of the VOC is an important task, the consequences resulting from a higher water content generate a spectrum of problems among which wettability of low surface tension substrates as well as stratification of polymer dispersions during their film formation is one of the primary concerns. A series of previous studies on latex films indicated that the mobility of low molecular weight species, in particular surfactant molecules, may be affected by latex glass transition temperature (T_g), and subsequently by the free volume of a polymer matrix,[1,2] surface tension at the film−air (F−A) and film−substrate (F−S) interfaces,[3−8] compatibility,[9−16] and coalescence times.[16−18] However, there are other factors that not only influence distribution of individual components, but may also significantly affect various stages of latex film formation. In an effort to elucidate the origin of this process and to enhance our understanding of the factors governing coalescence of blended and copolymer latexes, this study focuses on a series of experiments conducted on latex films containing controllable and well-defined quantities of styrene (Sty) and *n*-butyl acrylate (*n*-BA) moieties. While latex blends can be prepared by mixing independently polymerized *p*-Sty and p-*n*BA latex homopolymers in a form of polymeric microspheres dispersed in an aqueous medium, latex copolymers are synthesized by semicontinuous polymerization of Sty and *n*-BA monomers.[19] Although previous studies provided often speculative information pertaining to the effect of surfactant molecules as well as the latex film formation,[20] it is apparent that often common wisdom simplifies the actual physical phenomenon. Thus, present experiments focus on stratification of SDOSS in blended p-Sty and p-*n*BA latexes and copolymerized Sty/*n*BA latex films, and mechanisms of their film formation are discussed.

In an effort to spectroscopically establish surface distribution of sodium dioctylsulfosuccinate (SDOSS) surfactant molecules in 50/50% styrene/*n*-butyl acrylate (Sty/*n*-BA) copolymer latex and polymer blend films, molecular level probes will be utilized. While step-scan photoacoustic Fourier transform infrared (SS-PAS FT-IR) spectroscopy provides an opportunity for the surface depth profiling up to 150 μm,[21] attenuated total reflectance (ATR) FT-IR probes depths up to 3 μm, and quantitative information can be retrieved.[22] In an effort to determine surface morphology, FT-IR and FT-Raman microscopies can be utilized to visually assess and spectroscopically analyze latex surfaces. This combination of analytical tools is essential not only from the perspective of distribution of molecular entities across the surface and nondestructiveness of the measurements, but also makes vibrational microscopic techniques more accessible to nonspectroscopists. In this study, we will utilize FT-IR and FT-Raman imaging along with ATR FT-IR surface depth profiling in an effort to identify SDOSS surfactant distribution resulting from the film formation of 50/50% Sty/*n*-BA copolymer latexes and p-Sty/p-*n*BA polymer blends.

Experimental Section

Sample Preparation. A 50%/50% Sty/*n*-BA copolymer latex (particle size = 112 nm) was synthesized by a semicontinuous emulsion polymerization, as was described in the previous publications.[12,13] Liquid latex films (43 wt % solids) were cast on a polytetrafluoroethylene (PTFE) substrate and allowed to coalesce in air at 80% relative humidity (RH) for 3 days at room temperature. An approximate film thickness of dry films was 200 μm. Sty and *n*-BA monomers were individually polymerized following previously outlined procedures.[15] After synthesis of separate batches, p-Sty (particle size = 102 nm) and p-*n*BA (particle size = 150 nm) latexes, both 43 wt % solids homopolymer suspensions, were mixed in a 1:1 wt %

* To whom correspondence should be addressed.

† Work was potentially done at North Dakota State University. Parts I−XVI were published in *J. Appl. Polym. Sci.* (1990−1999).

10.1021/ma990559n CCC: $19.00
Published on Web 03/04/2000

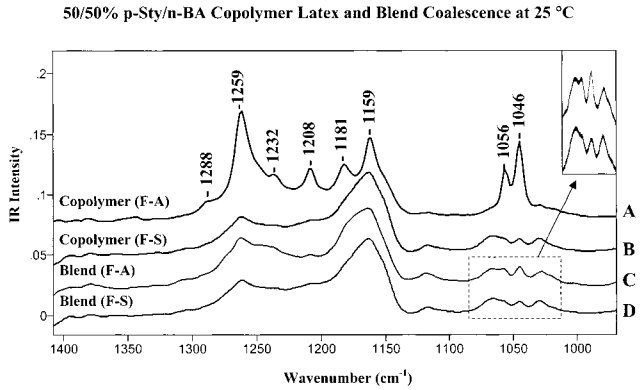

Figure 1. ATR FT-IR spectra in the 1340−970 cm^{-1} region of 50/50% Sty/*n*-BA copolymer and p-Sty/p-*n*BA blended latex films: A, copolymer F−A interface; B, copolymer F−S interface; C, blended latex F−A interface; D, blended latex F−S interface (coalescence time: 3 days, RH = 80%).

ratio, stirred, and stored for 10 days before allowed to coalesce under the above stated conditions.

Spectroscopic Measurements. ATR FT-IR spectra were collected on a Nicolet Magna-850 FT-IR single beam spectrometer at 4 cm^{-1} resolution and a mirror speed of 0.1581 cm s^{-1}. A KRS-5 crystal with a 45° angle 50 × 20 × 3 mm was used. Each spectrum represents 200 coadded scans ratioed to 200 scans collected on an empty ATR cell. All spectra were corrected for spectral distortions and optical effects using Q-ATR software.[22] Microscopic ATR FT-IR spectra were collected using the IRμs/Nic-Plan molecular microanalysis system (Nicolet Instruments, Inc.). Latex samples were analyzed using an ATR objective in a reflectance mode and equipped with a ZnSe crystal. Surfaces were mapped using a constant contact pressure between the ZnSe crystal and latex specimens. Each spectrum was recorded at 4 cm^{-1} resolution, and 200 scans were coadded using a 3.2 mm circular aperture. In a typical experiment, an ATR probe analyzes approximately 50−100 μm surface area and the source of an ATR signal comes from about 3 μm below the surface.[22]

SS-PAS FT-IR spectra were recorded on a Nicolet Magna 850 spectrometer equipped with a photoacoustic cell (MTEC Model 100, MTEC, Inc.). In a typical step-scan experiment, one scan was collected for 7198 s at a 8 cm^{-1} resolution. The spectra recorded at 1000, 750, 400, and 300 Hz modulation frequencies were collected with 0° and 90° phase angles, which are referred to as "I" (in-phase) and "Q" (in-quadrature) spectra, respectively.[23] To define 0° and 90° position with respect to the I and Q spectra, reference carbon black was used to set the phase angle for the strongest detector signal.[23] Since thermally thick carbon black absorbs almost all of the IR radiation, stronger peak-to-peak signals recorded from the SS-PAS spectrum are attributed to the surface of carbon black, and weaker signals are attributed to greater penetration depths. SS-PAS magnitude spectra were generated using the following relationship:[24] magnitude = $(I^2 + Q^2)^{1/2}$. Phase analysis spectra were generated using the following equation:[24] rotation = $I \cos \alpha + Q \sin \alpha$, where α is the phase angle. SS-PAS magnitude spectra illustrate information from estimated depths for a particular modulation frequency, whereas phase rotational analysis using I and Q spectra enhances spatial resolution for a given penetration depth.[24,25] All SS-PAS spectra were analyzed utilizing Omnic software.

Microscopic FT-Raman spectra were measured using an IFS 55/FRA 106 FT-IR/Raman spectrometer (Bruker Instruments, Inc.) from about 10 μm surface area. As an excitation source, a diode pumped Nd:YAG laser was used to provide a maximum power of 50 mW at the sampling area. Surface mapping was performed with a computerized *XY* stage in conjunction with the Opus mapping software (Bruker Instruments, Inc).

Dynamic Mechanical Thermal Analysis (DMTA). Glass transition temperatures (T_g) of latex films were measured using a dynamic mechanical thermal analysis instrument (Rheometric Scientific, DMTA 3E). Dry latex films were cut to 10 × 30 mm. The thickness of each specimen was approximately 200 μm. The DMTA scans were performed using a dynamic temperature ramp of 3 °C/min, a fixed oscillating

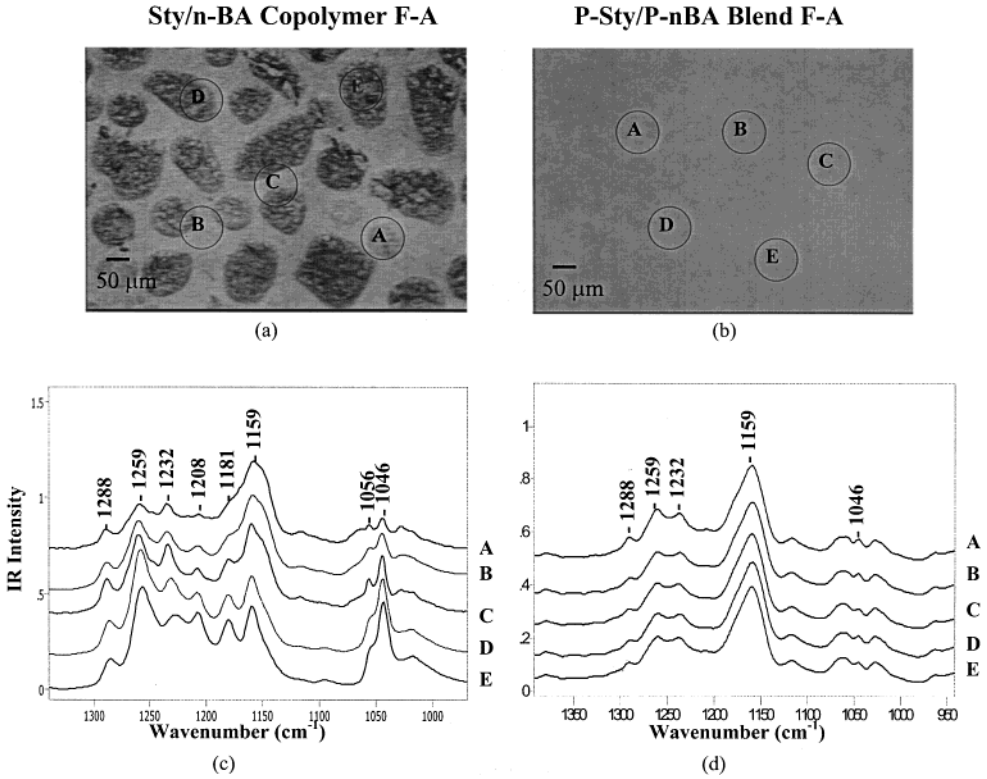

Figure 2. (a) Optical image of 50/50% Sty/*n*-BA copolymer latex F−A interface; (b) optical image of 50/50% p-Sty/p-*n*BA blended latex F−A interface; (c) ATR FT-IR spectra in the 1340−970 cm^{-1} region of 50/50% Sty/*n*-BA copolymer latex; (d) ATR FT-IR spectra in the 1400−940 cm^{-1} region of 50/50% p-Sty/p-*n*BA blended latex (coalescence time: 3 days, RH = 80%).

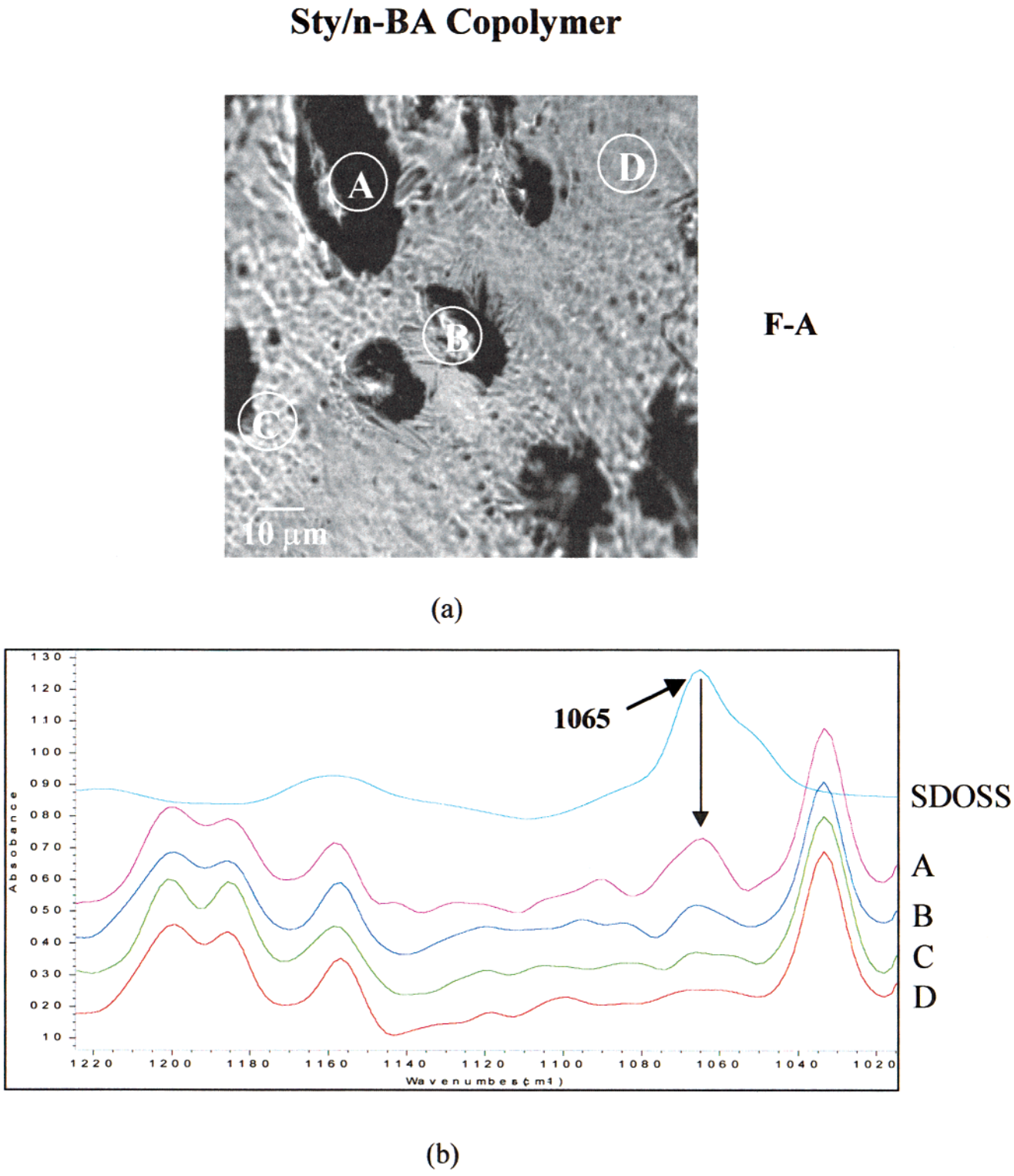

Figure 3. (a) Optical image of 50/50% Sty/*n*-BA copolymer latex F−A interface; (b) FT-Raman microscopic spectra in the 1220−1020 cm^{-1} region of Sty/*n*-BA copolymer F−A interface (coalescence time: 3 days, RH = 80%).

frequency of 1 Hz, and a controlled strain of 0.5% in the temperature range from −100 to 200 °C.

Results and Discussion

As indicated in the Introduction, our goal is to elucidate the origin of surfactant stratification and advance the still limited understanding of film formation processes in copolymer and polymer latex blends of p-Sty and p-*n*BA. Figure 1, traces A and B, illustrates ATR FT-IR spectra in the 1340−970 cm^{-1} region of coalesced Sty/*n*-BA copolymer latex films. The spectra were recorded from the F−A and F−S interfaces, respectively, at approximately 1.9 μm from each interface, and spectral distortions resulting from refractive index changes were corrected using Urban−Huang algorithm.[22] Although the total amount of SDOSS in the latex composition is 1.8 wt %, it is quite apparent that the F−A and F−S interfaces exhibit different and often accessible levels of SDOSS. As shown in trace A recorded from the F−A interface, the bands at 1288 and

1232 cm^{-1} are attributed to asymmetric stretching modes of H-bonded C−O−C species of SDOSS with COOH and H_2O, respectively.[3] On the other hand, the bands at 1259 and 1208 cm^{-1} are due to the S−O asymmetric stretching modes of the $SO_3^-Na^+\cdots COOH$ and $SO_3^-Na^+\cdots H_2O$ entities. Similarly, the 1056 and 1046 cm^{-1} bands are attributed to the S−O symmetric stretching modes resulting from $SO_3^-Na^+\cdots COOH$ and $SO_3^-Na^+\cdots H_2O$ interactions.[1−13] Trace B of Figure 1 illustrates an ATR spectrum recorded from the F−S interface, and it appears that the bands due to pure SDOSS and/or SDOSS associations are not detected. Thus, comparison of the spectra recorded from both interfaces indicate that, for Sty/*n*-BA copolymer latex, SDOSS exudes to the F−A interface.

Posponding temporarily the origin of surfactant exudation, let us now compare the above results with the data for p-Sty/p-*n*BA latex blends. In this case, p-Sty and p-*n*BA latexes were mixed in equal amounts and allowed to coalesce. Figure 1, traces C and D, shows ATR FT-IR spectra recorded from the F−A and F−S interfaces of p-Sty/p-*n*BA latex blend, respectively. As seen, only traces of the SDOSS bands at 1056 and 1046 cm^{-1} due to S−O symmetric stretching modes of $SO_3^-Na^+\cdots COOH$ and $SO_3^-Na^+\cdots H_2O$ associations[2−11] are detected at the F−A interface (trace C), but as compared to the F−S interface (trace D), they are stronger, indicating that only small quantities of SDOSS exude to the F−A interface. Overall, SDOSS bands at 1288, 1259, 1232, 1208, 1181, 1056, and 1046 cm^{-1} are significantly stronger in trace A than those in trace C, indicating that there is a greater degree of SDOSS accumulation near the F−A interface for copolymer latex than for its counterpart latex blend. Although all listed bands are attributed to SDOSS, our focus will be on the 1056 and 1046 cm^{-1} bands, as they are responsible for $SO_3^-Na^+\cdots COOH$ and $SO_3^-Na^+\cdots H_2O$ interactions, respectively.

While the above data show that SDOSS is present near the F−A interface, let us now determine surface/interfacial in-plane distributions of SDOSS molecules. Figure 2a,b shows optical images obtained from the F−A interfaces of copolymer and blended latex surfaces, respectively. As seen, aggregates are detected at the F−A interface of copolymer latex, whereas the F−A interface of latex blend appears to be uniform. In an effort to determine composition of aggregates detected in Figure 2a, ATR microanalysis was performed, which was accomplished by recording spectra using an ATR crystal on the surface area of 50−100 μm. While circles marked in Figure 2a,b indicate spectral acquisition areas at the F−A interfaces of copolymer and blended latex films, Figure 2c,d illustrates a series of spectra that correspond to points A, B, C, D, and E of Figure 2a,b, respectively. As seen in Figure 2c, the band at 1159 cm^{-1} due to the C−O−C stretching modes of p-*n*BA does not change its intensity, but the intensities of the 1056 and 1046 cm^{-1} bands due to SDOSS increase while moving an IR beam from points A through E. These results show that the observed aggregates in Figure 2a are mainly composed of water-soluble SDOSS islands. In contrast to the Sty/*n*-BA copolymer latex, SDOSS exhibits different behavior in p-Sty/p-*n*BA latex blends. As shown in Figure 2d, only traces of SDOSS are detected and the F−A interface (Figure 2b) appears to have uniform morphology.

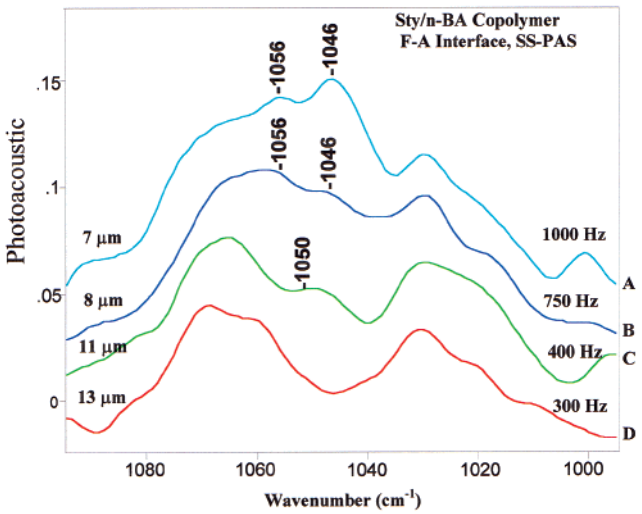

Figure 4. SS-PAS FT-IR magnitude spectra recorded at various modulation frequencies of 50/50% Sty/*n*-BA copolymer F−A interface (coalescence time: 3 days, RH = 80%): A, 1000 Hz; B, 750 Hz; C, 400 Hz; D, 300 Hz.

In an effort to establish if there is a detectable Sty/*n*-BA phase separation resulting from the SDOSS exudation to the surface in copolymer latex film, DMTA analysis was performed and a maximum of tan δ was used as a measure of the latex film glass transition temperature. The DMTA analysis (not shown) indicated that one maximum attributed to the glass transition temperature (T_g) at 20 °C of Sty/*n*-BA randomly copolymerized is present. This observation indicates that only spectroscopically detectable phase separation occurs between SDOSS and latex, but no phase separation within the copolymer latex components is present.

In an effort to confirm FT-IR results for copolymer latex film, FT-Raman images were recorded from both F−A and F−S interfaces. Similarly to FT-IR imaging, the F−S interface showed a smooth surface (not shown), but as seen in Figure 3a, an optical image of the Sty/*n*-BA copolymer F−A interface appears to show nonuniformly distributed islands. Figure 3b represents a series of FT-Raman spectra recorded from points A, B, C, and D of Figure 3a. As seen, the intensity of the band at 1065 cm^{-1} due to S−O symmetric stretching modes of SDOSS decreases while going from point A to D. These results confirm FT-IR imaging experiments illustrated in Figure 2a,c and indicate again that SDOSS islands result from the migration of SDOSS to the surface. It should be noted that images shown in Figures 2 and 3 exhibit slightly different appearance because different illumination conditions and magnification were utilized in Raman and FT-IR microscopy experiments.

So far we have shown that SDOSS molecules of Sty/*n*-BA copolymer latex exude to the F−A interface, and stratify near the surface forming nonuniformly distributed islands. In contrast, stratification in p-Sty/p-*n*BA latex blends is minimal. The next issue of importance is to determine relative distribution of SDOSS molecules in the direction perpendicular to the F−A and F−S interfaces. For this reason SS-PAS FT-IR spectra were recorded from the Sty/*n*-BA copolymer latex F−A interface. Figure 4, traces A−D, illustrates a series of SS-PAS FT-IR magnitude spectra recorded at 1000, 750, 400, and 300 Hz modulation frequencies. These frequencies correspond to approximate penetration depths

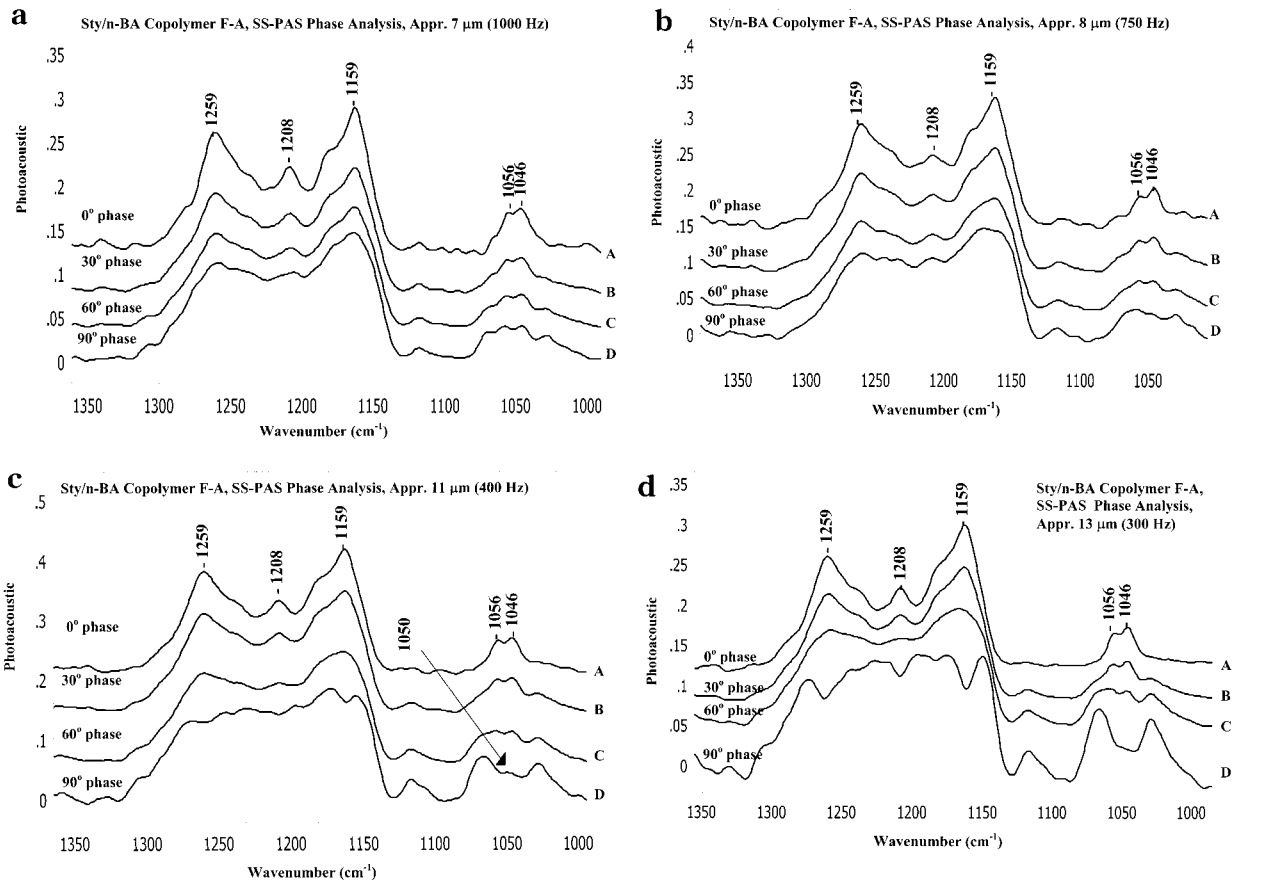

Figure 5. Four steps of SS-PAS FT-IR spectra recorded at various modulation frequencies with I (0°) and Q (90°) phase angles near the 50/50% Sty/*n*-BA copolymer F−A interface: (a) 1000 Hz; (b) 750 Hz; (c) 400 Hz; (d) 300 Hz.

of 7, 8, 11, and 13 μm.[24] As we recall, the bands at 1056 and 1046 cm^{-1} (trace A) result from the $SO_3^-Na^+\cdots$ COOH and $SO_3^-Na^+\cdots H_2O$ entities, and the band intensities resulting from these interactions decrease while going from 7 (trace A) to 8 μm (trace B). At 11 μm from the F−A interface (trace C), only the 1050 cm^{-1} band due to nonbonded $SO_3^-Na^+$ hydrophilic end groups on SDOSS is detected. In contrast, at 13 μm from the surface (trace D), no SDOSS is detected. The presence of the 1056 and 1046 cm^{-1} bands detected at about 8 μm from the surface, and the 1050 cm^{-1} band detected near 11 μm into the F−A interface, indicate that SDOSS molecules form SDOSS$\cdots H_2O$ and SDOSS$\cdots$COOH associations at about 7−8 μm below the surface, and the nonbonded SDOSS is present at about 11 μm.

In an effort to enhance spatial normal-to-the-surface resolution in a photoacoustic detection, phase rotation analysis using I and Q spectra was performed.[24,25] This approach allows analysis of spectral features below the surface without being affected by what is above, and recent studies demonstrated this useful capability.[26] Figure 5 shows four steps in the SS-PAS FT-IR phase analysis spectra recorded from 7, 8, 11, and 13 μm, respectively. Traces A, B, C, and D of each figure represent I (0°), 30°, 60°, and Q (90°) spectra. As seen in Figure 5a, the presence of SDOSS$\cdots H_2O$ associations is demonstrated by the detection of the bands at 1046 and 1208 cm^{-1}, which decrease while going from 0° to 90°. However, the bands at 1056 and 1259 cm^{-1} due to SDOSS$\cdots$COOH interactions remain constant. At about 8 μm from the F−A interface (Figure 5b), while going from 0° to 90°, the 1046 and 1208 cm^{-1} band intensities due to SDOSS$\cdots H_2O$ and 1056 and 1259 cm^{-1} due to

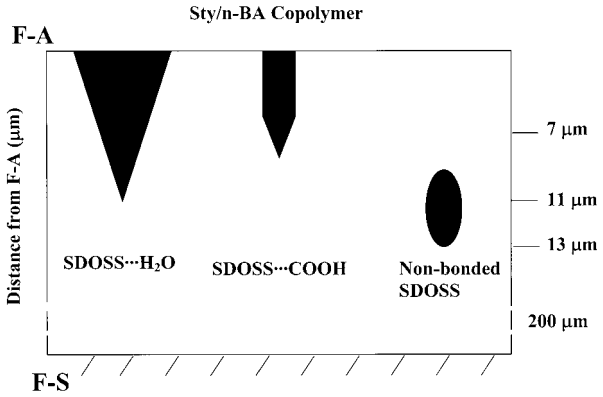

Figure 6. Schematic diagram of relative quantities of SDOSS associated with H_2O, COOH, and nonbonded SDOSS as a function of the depth penetration from 50/50% Sty/*n*-BA copolymer F−A interface.

SDOSS$\cdots$COOH decrease. When the signal comes from about 11 μm below the surface (Figure 5c), for the same phase angle changes, the band intensities at 1259, 1208, 1046, and 1056 cm^{-1} also decrease. These results indicate that the Q spectrum (trace D) shows no bands due to SDOSS$\cdots H_2O$ and SDOSS$\cdots$COOH entities, but free $SO_3^-Na^+$ hydrophilic end groups (1050 cm^{-1}) are detected. Based on the results presented in Figures 1−5, Figure 6 was constructed, which schematically illustrates distribution of SDOSS molecules across the Sty/*n*-BA copolymer latex film thickness. Although at this point it is apparent that the magnitude and the character of SDOSS interactions change as a function of depth, the origin of these interactions as a function of depth is yet to be established.

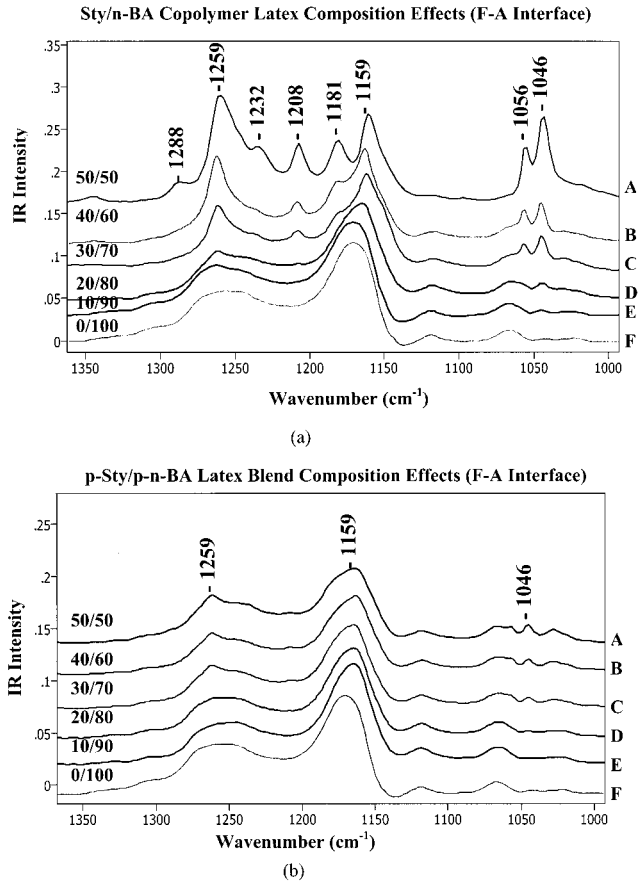

Figure 7. (a) ATR FT-IR spectra in the 1370−970 cm^{-1} region of copolymer latex F−A interface with composition effects: A, 50/50%; B, 40/60%; C, 30/70%; D, 20/80%; E, 10/90%; F, 0/100%. (b) ATR FT-IR spectra in the 1370−970 cm^{-1} region of blended latex F−A interface with composition effects: A, 50/50%; B, 40/60%; C, 30/70%; D, 20/80%; E, 10/90%; F, 0/100% (coalescence time: 3 days, RH = 80%).

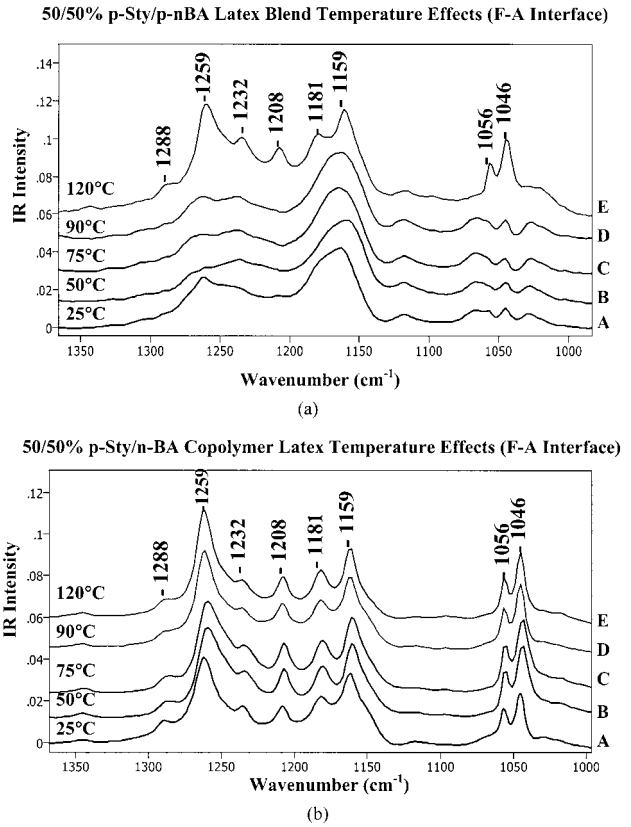

Figure 8. (a) ATR FT-IR spectra in the 1360−970 cm^{-1} region of various compositions of p-Sty/p-*n*BA blended latex with annealing temperature effects: A, 25 °C; B, 50 °C; C, 75 °C; D, 90 °C; E, 120 °C. (b) ATR FT-IR spectra in the 1360−970 cm^{-1} region of various compositions of Sty/*n*-BA copolymer latex with annealing temperature effects: A, 25 °C; B, 50 °C; C, 75 °C; D, 90 °C; E, 120 °C.

As we recall, DMTA results for the latex copolymer exhibits T_g of 20 °C. However, for p-Sty/p-*n*BA latex blend, two T_g's are detected at −35 and 110 °C, which are due to phase separation of p-*n*BA and p-Sty, respectively. Although this observation is not surprising, the next question to be addressed is how the presence of two separated p-Sty and p-*n*BA phases may affect surfactant behavior during latex film formation. Previous studies[10,27,28] showed that surfactant molecules may be largely, if not completely, displaced from latex particle surfaces due to significant interdiffusion of polymeric particle segments during latex coalescence. Furthermore, surfactant mobility can be also significantly influenced by a composition of latex particles. For higher Sty content in Sty/*n*-BA copolymer latex, enhanced SDOSS migration to the F−A interface was detected and attributed to the diminished compatibility between SDOSS and Sty/*n*-BA copolymer.[1] For p-Sty, p-*n*BA, and SDOSS, compatibility between p-Sty/SDOSS and p-*n*BA/SDOSS can be estimated using three-dimensional solubility parameters δ.[29] Using the literature solubility parameters[30] for p-Sty (δ_d = 9.09 $(cal/cm^3)^{1/2}$, δ_p = 2.1 $(cal/cm^3)^{1/2}$) and p-*n*BA (δ_d = 6.90 $(cal/cm^3)^{1/2}$, δ_p = 5.2 $(cal/cm^3)^{1/2}$), one can estimate the magnitude of interactions between SDOSS molecules and polymers. For SDOSS [$C_8H_{17}CO_2CH_2CH(SO_3^-Na^+)CO_2C_8H_{17}$], solubility parameters can be estimated from the volume fraction contributions of polar and nonpolar segments which are δ_d = 5.62 $(cal/cm^3)^{1/2}$ and δ_p = 10.5 $(cal/cm^3)^{1/2}$,[29] respectively. Because the difference between the δ_d and δ_p values for p-*n*BA/SDOSS is smaller than that for p-Sty/SDOSS, higher compatibility for p-*n*BA/SDOSS pairs is expected which supports the spectroscopic data.

In an effort to experimentally confirm that the latex−SDOSS compatibility is responsible for stratification of SDOSS, Sty/*n*-BA copolymer was prepared at different weight percent Sty/*n*-BA ratios. A premise behind this experiment is that for a higher Sty content in a Sty/*n*-BA copolymer, more SDOSS will exude to the F−A interface. ATR FT-IR spectra of 50/50, 40/60, 30/70, 20/80, 10/90, and 0/100 wt % Sty/*n*-BA copolymer latexes are shown in Figure 7a, traces A−F, respectively. As shown by the enhanced intensities of the SDOSS bands, increased Sty content in the copolymer latex increases the amount of SDOSS diffusing to the F−A interface. Again, ATR FT-IR spectra were recorded from 1.9 μm from the F−A interface and all spectra were corrected for optical distortions. Thus, these results confirm that p-*n*BA/SDOSS pairs exhibit stronger compatibility in contrast to their p-Sty/SDOSS counterparts. As a result, SDOSS is expelled from the copolymer latexes containing higher Sty content.

At this point one would like to compare these results with the latex blend containing p-Sty and p-*n*BA latexes. Figure 7b, traces A−F, illustrates p-Sty/p-*n*BA blend ATR FT-IR spectra which do not exhibit intensity changes resulting from the p-Sty/p-*n*BA compositional changes. Although these results explicitly show that p-Sty and p-*n*BA latex blends provide more compatible

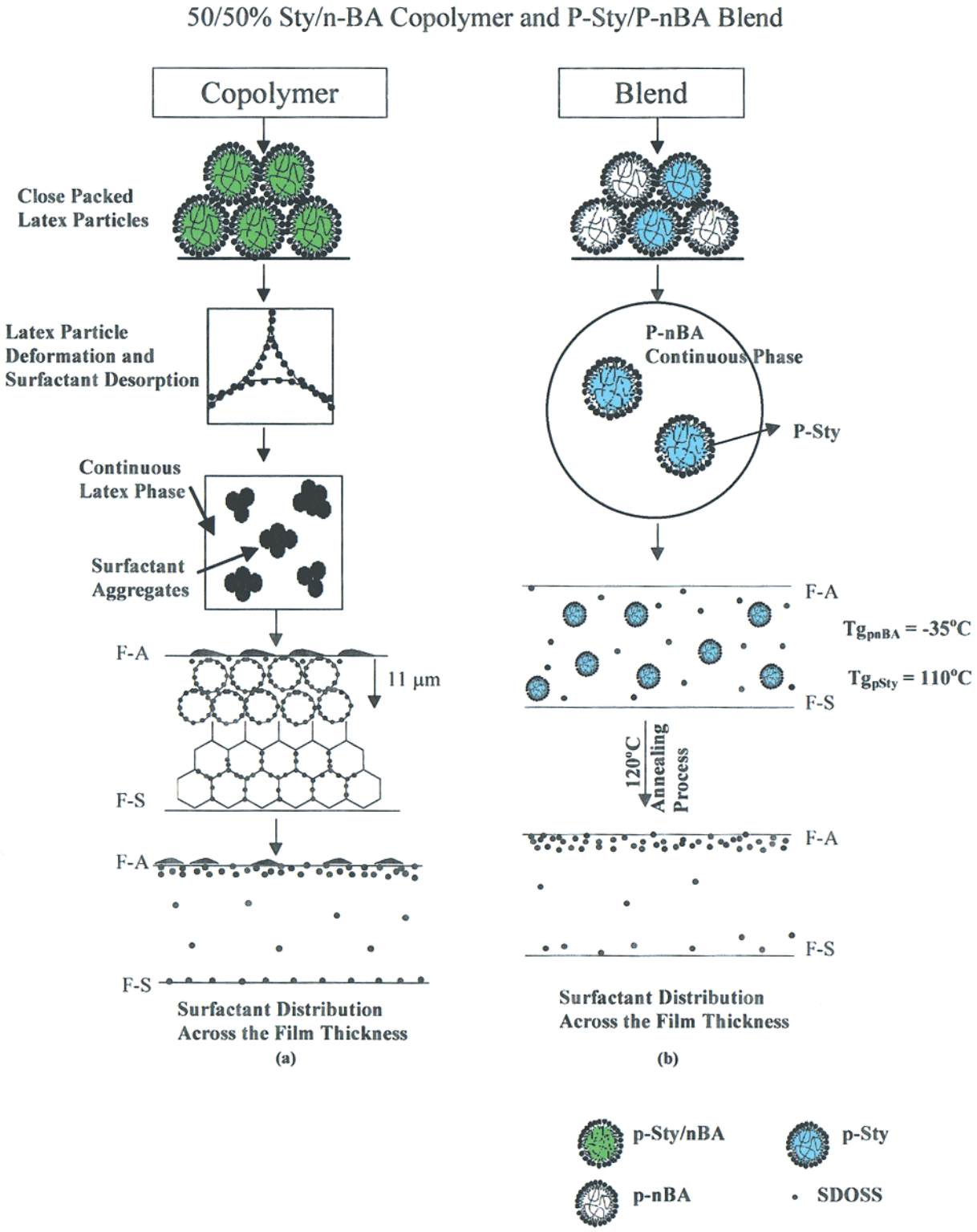

Figure 9. Schematic diagrams illustrating film formation and surfactant behavior in different latex systems: (a) 50/50% Sty/*n*-BA copolymer latex; (b) 50/50% p-Sty/p-*n*BA latex blend.

environments for SDOSS, these results are somewhat surprising because one would anticipate that the presence of p-Sty particles, which are less compatible with SDOSS, should enhance the SDOSS separation from a p-Sty/p-*n*BA polymer blend.

Since the temperature difference between coalescence and the actual T_g of the latex appears to have a significant effect on coalescence, and thus may influence migration of SDOSS, the latex films were annealed at 50, 75, 90, and 120 °C for 2 h, followed by cooling to 25 °C. Traces A, B, C, D, and E represent ATR FT-IR spectra of 50/50% p-Sty/p-*n*BA blend (Figure 8a) and 50/50% Sty/*n*-BA copolymer latex (Figure 8b) films annealed at 25, 50, 75, 90, and 25 °C. As seen in Figure 8a for the latex blend, the bands at 1046 and 1056 cm^{-1} are significantly enhanced when annealing temperatures reach 120 °C (trace E), as opposed to 25 °C (trace A). Furthermore, only slight intensity increases are detected at 90 °C (trace D). These results show that SDOSS migration to the F−A interface is significantly

enhanced when the annealing temperature is above p-Sty T_g (110 °C), thus implying that coalescence of p-Sty particles at 120 °C results in expelling SDOSS molecules from the latex blend system due to lower p-Sty/SDOSS compatibility. However, enhanced free volume of the p-Sty phase above the T_g may be also a containing factor that accelerates migration of SDOSS. In contrast, for 50/50% Sty/*n*-BA copolymer latex, the band intensities at 1046 and 1056 cm^{-1} (Figure 8b) are temperature independent (traces A−E).

Based on these results, a schematic diagram illustrating 50/50% Sty/*n*-BA copolymer and p-Sty/p-*n*BA blend film formation was constructed. As shown in Figure 9a, for 50/50% Sty/*n*-BA copolymer latex with $T_g = 20$ °C and coalesced at 25 °C, film formation involves water evaporation, which leads to a closer particle packing. The presence of the band at 1046 cm^{-1} detected at 11 μm (Figure 6) indicates that SDOSS···H_2O associations are present at this depth. Due to the fact that SDOSS is mobile, it is likely that they occur at the particle interstices, as the interparticle diffusion is not complete. The presence of surfactant aggregates detected at the F−A interface indicates phase separation between SDOSS and the latex copolymer which occurs due to relatively poor compatibility and competing water flux driving low molecular weight species to the F−A interface. Excessive concentration levels of SDOSS at the F−A interface also suggest that most surfactant molecules migrate to the surface and, as coalesence continues, relatively small amounts of surfactant molecules are dispersed in the coalesced latex matrix. For 50/50% p-Sty/p-*n*BA blended latexes coalesced at 25 °C, the film formation process is shown in Figure 9b and involves water evaporation from the dispersion, followed by a close packing of p-*n*BA particles which deform to flow around hard p-Sty particles.[31] In contrast to Sty/*n*-BA copolymer, no SDOSS stratification is detected when blended latex is coalesced at 25 °C, which indicates that surfactant molecules are imbedded in the p-Sty particle surfaces. However, after annealing at 120 °C, SDOSS molecules migrate to the F−A interface, which indicates that SDOSS is released from the p-Sty particles when coalescence temperatures are above the T_g of p-Sty phase. The question that remains to be answered is whether the entrapment of SDOSS on p-Sty particles is caused by relative to p-*n*BA smaller free volume of p-Sty below its T_g, thus not allowing hydrophobic ends of SDOSS to be released, or the extent of p-Sty−SDOSS hydrophobic interactions. Although the presented data do seem to point toward the free volume effect, further experiments[32] are necessary to relate the extent of hydrophobic interactions with the free volume changes at elevated temperatures.

Conclusions

These studies show that ATR FT-IR and FT-Raman microscopies as well SS-PAS FT-IR can be effectively utilized to study surfactant stratification during Sty/*n*-BA copolymer and polymer blend latex film formation. For copolymer latex, SDOSS aggregates are detected at the F−A interface and their concentration is significantly higher as compared to the F−S interface. SS-PAS FT-IR spectroscopy allows us to monitor surfactant distribution across the film thickness. These studies show that SDOSS···H_2O, SDOSS···COOH, and non-bonded SDOSS species exist at various depths from the F−A interface. While SDOSS molecules are uniformly distributed at the F−A interface of latex blend, their concentration levels are much smaller in copolymer latex. The glass transition temperature of latex also significantly affects exudation of SDOSS, especially when the coalescence temperature is above the T_g.

Acknowledgment. The authors are thankful to the National Science Foundation Industry/University Cooperative Research Center in Coatings for financial support of these studies.

References and Notes

(1) Niu, B.-J.; Urban, M. W. *J. Appl. Polym. Sci.* **1995**, *56*, 377.
(2) Niu, B.-J.; Urban, M. W. *J. Appl. Polym. Sci.* **1996**, *60*, 371.
(3) Urban, M. W.; Evanson, K. W. *Polym. Commun.* **1990**, *31*, 279.
(4) Thorstenson, T. A.; Evanson, K. W.; Urban, M. W. *Polym. Mater. Sci. Eng.* **1991**, *64*, 195.
(5) Thorstenson, T. A.; Tebelius, L. K.; Urban, M. W. *J. Appl. Polym. Sci.* **1993**, *49*, 103.
(6) Evanson, K. W.; Thorstenson, T. A.; Urban, M. W. *J. Appl. Polym. Sci.* **1991**, *42*, 2309.
(7) Thorstenson, T. A.; Evanson, K. W.; Urban, M. W. *Advances in Chemistry Series*; Urban, M. W., Craver, C. D., Eds.; American Chemical Society: Washington, DC, 1993; No. 236.
(8) Evanson, K. W.; Urban, M. W. *Surface Phenomena and Fine Particles in Water-based Coating and Printing Technology*; Sharma, M. K., Micale, F. J., Eds.; Plenum: New York, 1991, 197.
(9) Thorstenson, T. A.; Urban, M. W. *J. Appl. Polym. Sci.* **1993**, *47*, 1387.
(10) Thorstenson, T. A.; Urban, M. W. *J. Appl. Polym. Sci.* **1993**, *50*, 1207.
(11) Niu, B.-J.; Urban, M. W. *J. Appl. Polym. Sci.* **1996**, *60*, 389.
(12) Evanson, K. W.; Thorstenson, T. A.; Urban, M. W. *J. Appl. Polym. Sci.* **1991**, *42*, 2297.
(13) Evanson, K. W.; Urban, M. W. *J. Appl. Polym. Sci.* **1991**, *42*, 2287.
(14) Kunkel, J. P. W.; Urban, M. W. *J. Appl. Polym. Sci.* **1993**, *50*, 1217.
(15) Tebelius, L. K.; Urban, M. W. *J. Appl. Polym. Sci.* **1995**, *56*, 387.
(16) Zhao, C. L.; Holl, Y.; Pith, T.; Lambla, M. *Colloid Polym. Sci.* **1987**, *265*, 823.
(17) Thorstenson, T. A.; Urban, M. W. *J. Appl. Polym. Sci.* **1993**, *47*, 1381.
(18) Niu, B.-J.; Urban, M. W. *J. Appl. Polym. Sci.* **1996**, *60*, 379.
(19) Ramarai, B; Rajalingam, P.; Radhakrishnan, G. *J. Appl. Polym. Sci.* **1991**, *43*, 23.
(20) Du Chesne, A.; Gerharz, B.; Lieser, G. *Polym. Int.* **1997**, *43*, 187−196.
(21) Rosencwaig, A. *Photoacoustic and Photoacoustic Spectroscopy*; John Wiley and Sons: New York, 1980.
(22) Urban, M. W. *Attenuated Total Reflectance Spectroscopy of Polymers−Theory and Practice*; American Chemical Society: Washington, DC, 1996.
(23) Niu, B.-J.; Urban, M. W. *Film Formation in Waterborne Coatings*; Provder, T., Winnik, M. A., Urban, M. W., Eds.; American Chemical Society: Washington, DC, 1996; pp 319−331.
(24) Jones, R. W.; Mcclelland, J. F. *Appl. Spectrosc.* **1996**, *50*, 1258−1262.
(25) Jiang, E. Y.; Palmer, A. P.; Barr, N. E. *Appl. Spectrosc.* **1997**, *51*, 1238−1244.
(26) Stegge, J.; Urban, M. W. *Science* **2000**, in press.
(27) Wicks, Z. W.; Jones, F. N.; Pappas, S. P. *Org. Coat.: Sci. Technol.* **1992**, *1*, 46−48.
(28) Chevalier, Y.; Pichot, C.; Graillat, C.; Joanicot, M.; Wong, K.; Maquet, J.; Lindner, P.; Cabane, B. *Colloid Polym. Sci.* **1992**, *270*, 806.
(29) Little, R. C. *J. Colloid Interface Sci.* **1978**, *65*, (3).
(30) Grulke, E, A. *Polymer Handbook*, 3rd ed.; Wiley Interscience: New York, 1989; pp VII/519−VII/557.
(31) Keddie, J. L.; Meredith, P.; Jones, R. L.; Donald, A. M. *Langmuir* **1996**, *12*, 3793.
(32) Studies in progress.

MA990559N